

Dendrons

Poly(aryl ether) Dendrons with Monopyrrolotetrathiafulvalene Unit-Based Organogels exhibiting Gel-Induced Enhanced Emission (GIEE)

Yucun Liu, Wenwei Lei, Tie Chen,* Longyi Jin, Guangyan Sun, and Bingzhu Yin*^[a]

Abstract: A series of poly(aryl ether) dendrons with a monopyrrolo-tetrathiafulvalene unit linked through an acyl hydrazone linkage were designed and synthesized as low molecular mass organogelators (LMOGs). Two of the dendrons could gelate the aromatic solvents and some solvent mixtures, but the others could not gel all solvents tested except for *n*-pentanol. A subtle change on the molecular structure produces a great influence on the gelation behavior. Note that the dendrons could form the stable gel in the DMSO/water mixture without thermal treatment and could also form the binary gel with fullerene (C₆₀) in toluene. The formed gels undergo a reversible gel-sol phase transition upon exposure to external stimuli, such as temperature and

chemical oxidation/reduction. A number of experiments (SEM, FTIR spectroscopy, ¹H NMR spectroscopy, and UV/Vis absorption spectroscopy, and XRD) revealed that these dendritic molecules self-assembled into elastically interpenetrating one-dimensional fibrillar aggregates and maintain rectangular molecular-packing mode in organogels. The hydrogen bonding, π - π , and donor-acceptor interactions were found to be the main driving forces for formation of the gels. Moreover, the gel system exhibited gel-induced enhanced emission (GIEE) property in the visible region in spite of the absence of a conventional fluorophore unit and the fluorescence was effectively quenched by introduction of C₆₀.

Introduction

The construction of functional materials through the bottom-up approach associated with molecular self-assembly allows the translation of information from the molecular scale into materials with specific functions.^[1] Over the last decade, supramolecular gels,^[2] representing one of the most important soft materials, have attracted widespread attention because of their potential applications in drug delivery,^[3] tissue engineering,^[4] sensors and actuators,^[5] template materials,^[6] removal of pollutants,^[7] enzyme immobilization matrices,^[8] catalysis,^[9] and crystal growth,^[10] using noncovalent interactions (hydrogen bonding, π - π interactions, metal-ligand coordination, van der Waals forces, London dispersion forces, donor-acceptor interactions and hydrophobic effects) for forming nanofibrillar structures able to "freeze" solvents in the rigid gel framework.^[11] Among them, low-molecular mass organogelators (LMOGs) can be cross-linked into different 3D self-assembled blocks, such as fibers, rods, ribbons, or other morphologies, through noncovalent interactions. Because of the weak nature of these forces, the gel-solution (gel-sol) transition for organo-

gels is thermally reversible and can be further tuned by other physical and chemical stimuli.

So far, a number of physically thermoreversible hydrogel and organogel systems that consist of gelators with different functionalities have been reported.^[12] Self-assembly in dendrimers has been intensively investigated because of their potential candidacy in soft matter chemistry and numerous structural patterns have already been recognized in this regard.^[13] As a new kind of LMOGs, organogelators based on dendrimers and/or dendrons have also attracted much interest because of the advantages of significant steric impact and their ability to form multiple noncovalent interactions.^[14] In 2000, Aida and co-workers reported the first example of a dendritic organogel by using ester-terminated Fréchet-type dendrons with a dipeptide at the focal point.^[15] Since then, Zhang and Fan described the self-assembly of tetraphenylethene, perylenediimide, and spiropyran-functionalized poly(aryl ether) dendron derivatives to a photoresponsive organogel.^[16] Recently, Prasad and co-workers reported a series of robust gel systems generated from poly(aryl ether) dendrons with anthracene, pyrene, glucose, naphthalene and pyridine units attached through an acyl hydrazone linkage, which own "tunable" morphology or light-emitting properties.^[17] Interestingly, a poly(aryl ether) dendron with a ferrocene unit-based organogelator could self-assemble to form a redox-responsive gel.^[18] From these advances, it is clear that the combination of Fréchet-type dendron and acyl hydrazone unit are capable of forming a large number of intermolecular interactions through π - π and hydrogen-bonding networks, leading to gels with relatively low critical gel

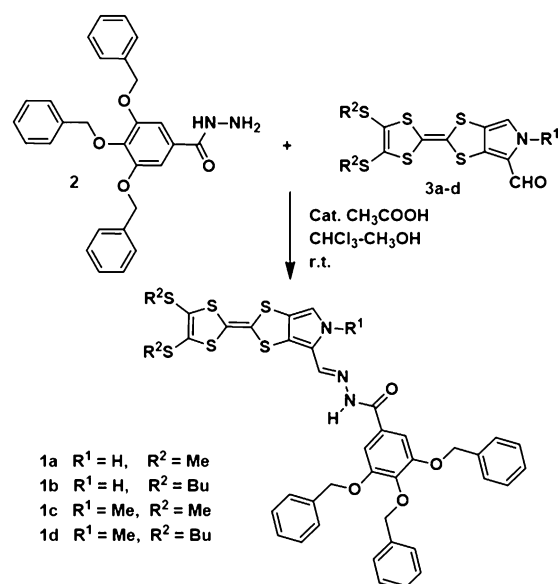
[a] Dr. Y. Liu, W. Lei, Prof. T. Chen, Prof. L. Jin, G. Sun, Prof. B. Yin
Key Laboratory of Natural Resources of Changbai Mountain & Functional Molecules of Ministry of Education
Yanbian University, Yanji, Jilin 133002 (P.R. China)
Fax: (+86)433-2732456
E-mail: zqcong@ybu.edu.cn

Supporting information for this article is available on the WWW under <http://dx.doi.org/10.1002/chem.201502044>.

concentration (CGC) values and the gel systems have many potential applications. In spite of the numerous applications of poly(aryl ether) dendron compounds in material chemistry, it remains a great challenge to design effective dendron organogelators, especially those with an electron-donating group.

Functional organogels containing electroactive units have drawn significant attention as these supramolecular structures have been the focus of immense interest in optoelectronic applications.^[19] Tetrathiafulvalene (TTF) is a redox-active compound that can exist in three redox states (TTF⁰, TTF⁺, TTF²⁺). Because of this property, TTF and its π -extended derivatives are particularly interesting as redox-active units in molecular electronics devices, with the possibility to switch between conducting ON–OFF states by applying, for example, a high bias potential or an external gating potential.^[20] On the basis of this view, researchers have established that the ability of the TTF core to act as a redox-active subunit is because of its ability to self-assemble in solution and in the solid state.^[21] Recently, TTFs have been employed as building blocks for molecular devices such as organic field-effect transistors,^[22] liquid crystalline materials,^[23] sensors,^[24] molecular switches,^[25] conductive material,^[26] nonlinear optical devices,^[27] rectifiers,^[20b] and organic photovoltaic cells.^[28] Based on TTF's good electron-donating ability and reversible one-electron oxidation action, LMOGs with TTF units have received considerable attention. In 1994, the self-assembled molecular wires of a TTF gel were first introduced by Jørgensen and co-workers.^[29] Since then, a number of physically thermoreversible organogel systems based on TTF unit with different chemical structures and functional groups have been reported. For example, Becher et al. constructed oriented nanowires and organogels based on amphiphilic TTF-substituted macrocycles.^[30] Zhu et al. utilized the redox properties of the TTF moiety to tune the gel–sol transition behaviors.^[31] After then, this group reported a new TTF-based molecular gelator with a dendron substituent, in which the TTF unit could be oxidized into TTF⁺ by chloranil in the presence of either Sc³⁺ or Pb²⁺.^[32] Recently, our group have explored the multiple stimulus responsive organogels based on monopyrrolotetrathiafulvalene (MPTTF) with different number of amide units and its CT complex.^[33] Incredibly, although a large number of organogelators based on TTF units have emerged, to our knowledge, the TTFs-linked dendron organogels have not been reported yet.

Herein, we report a series of poly(aryl ether) dendrons with an electroactive MPTTFs unit linked through an acyl hydrazone linkage as organogelators (Scheme 1). As always, the MPTTF core acts as a redox and electron-donating center in the gel system and provides S...S and π – π interactions. The combination of a MPTTF unit and a poly(aryl ether) dendron through an acyl hydrazone linkage will result in the gelation through intermolecular π – π and S...S interactions. In addition, the acyl hydrazone linkage provides hydrogen-bonding interactions to promote the gelation of the dendrons. The present dendrons could efficiently gelate aromatic solvents such as benzene, toluene, chlorobenzene, and xylene, and some solvent mixtures. The gelation leads to fine fibrillar type aggregates, which interestingly exhibits a gelation induced emission in the visible



Scheme 1. Molecular structures and synthetic route of the dendrons 1 a–d.

region, despite the absence of a conventional fluorophore unit,^[17b] and the fluorescence intensity was quenched by fullerene (C₆₀) in the gel system.

Results and Discussion

Synthesis and gelation

The starting and intermediate compounds **2**, **3 b**, and **3 d** were synthesized according to the previous reported procedures^[17e,34] (see the Supporting Information). Target dendrons were synthesized by an aldimine condensation of 3,4,5-tris(benzyloxy) benzohydrazide (**2**) with corresponding MPTTF carbaldehydes (**3 a**, **3 b**, **3 c**, and **3 d**) in very good yields. For comparison purposes, we tuned the length of the alkyl chain of the attached TTF skeleton and the substituent on the nitrogen of pyrrole ring. The chemical structures and purities of all newly synthesized compounds were characterized by ¹H NMR, ¹³C NMR spectroscopy and MALDI-TOF mass spectrometry (the detailed synthetic procedure and spectral data are given in the Supporting Information).

The gelation ability of dendrons **1 a–1 d** was studied in a variety of organic solvents as well as solvent mixtures by “stable to inversion of glass vial”. The critical gel concentration (CGC) values of the dendrons were determined in each solvent and the results are given in Table S1 (the Supporting Information). As seen in Table S1 (the Supporting Information), the dendrons are easily soluble in the polar aprotic solvents (such as THF, DMF, DMSO, CHCl₃, and so on) but insoluble in saturated hydrocarbon and protic solvents (such as *n*-hexane, cyclohexane, methanol, and ethanol). The gelation behaviors of dendrons **1 a–1 b** and **1 c–1 d** are different: dendrons **1 a** and **1 b** could gel aromatic solvents (such as benzene, toluene, xylene, and chlorobenzene) to form the thermo-reversible opaque yellow organogels and possess low critical gelation concentrations in

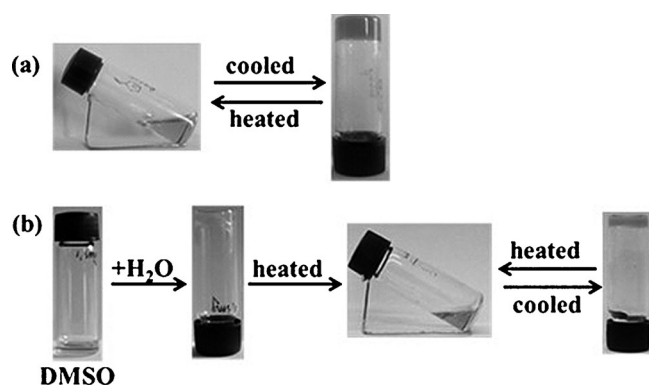


Figure 1. Photographs of sol-gel transition of **1b** in toluene (a) and the mixture of DMSO/water (2:1) (b).

the measured solvents. For instance, the gelation of 1 mL of toluene requires 1.6 mg of **1a** and 1.5 mg of **1b**, respectively (Figure 1a and Table S1, the Supporting Information). Moreover, dendrons **1a** and **1b** could also form a gel in solvent mixtures. For example, addition of *n*-hexane to a chloroform solution of the dendrons leads to the formation of an opaque organogels (Figure S1, the Supporting Information). Interestingly, compounds **1a** and **1b** form translucent gels when added water to their DMSO solution without heating and cooling treatment. Furthermore, these translucent gels could change to opaque organogels upon heating and cooling process, and are thermo-reversible in nature (Movie 1 (the Supporting Information) and Figure 1b). By comparison with **1a** and **1b**, dendrons **1c** and **1d**, each of which has a methyl group on nitrogen of pyrrole ring in dendron molecule, could not gel all solvents tested except for *n*-pentanol. A subtle change on the molecular structure produces a great influence on the gelation ability. The larger solubility and low gelation ability of **1c** and **1d** than **1a** and **1b** in the solvents suggest that the intermolecular interaction between **1c** or **1d** is weaker than that between **1a** or **1b**. It is clear that the intra- or intermolecular hydrogen bonding from the hydrogen atom on the nitrogen atom of the pyrrole ring play a key role.

To investigate the thermal stability of the resulting gels, the gel-sol phase transition temperatures (T_{gel}) were measured at different concentrations of the gelators by a convenient ball-drop method. As shown in Figure 2, the T_{gel} value increased with increasing gelator concentration due to the increasing participation of intermolecular noncovalent interactions. The T_{gel} values of **1a** and **1b** in benzene varied from 56 to 80 °C for **1a** and 51 to 80 °C for **1b** at their CGC, indicating that the gel systems had stable supramolecular structures at this concentration and good thermal stability.

Morphologies and architectures

The dendron in the gel phase were initially examined by using optical microscopic techniques.^[18,35] The optical microscope images of the gels of **1a** and **1b** obtained from the mixture of DMSO/water with and without thermal treatment were depicted in Figure 3. The aggregation in all gel phases shows fibrous

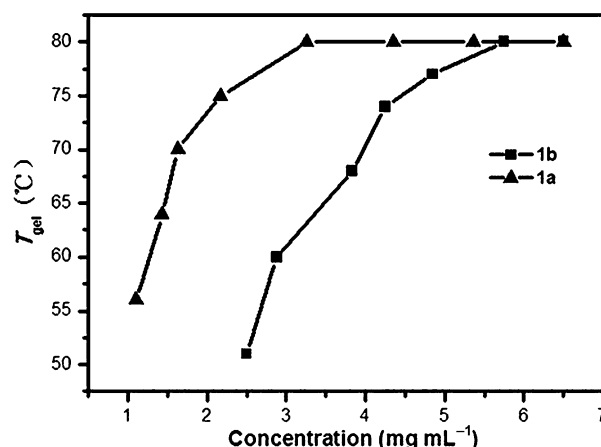


Figure 2. Variation of the T_{gel} of organogels of **1a** and **1b** with increasing gelator concentration in benzene.

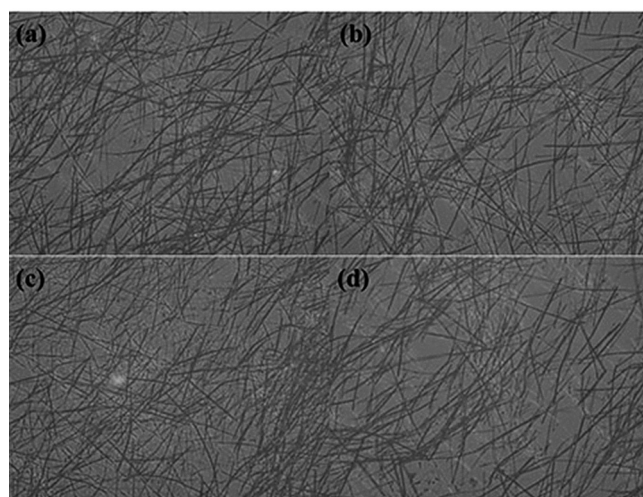


Figure 3. Optical microscopic images of the xerogels (a) **1a** and (b) **1b** with or (c) **1a** and (d) **1b** without thermal treatment from DMSO/water (2:1, v/v) (100× magnification).

crystallites with a well-defined uniform fiber-type self-assembly. To gain a detailed insight into the gelation behavior and nature of the self-assembly, the morphology of xerogels of gelators **1a** and **1b** was observed through scanning electron microscopy (SEM). As seen in Figure 4a and b, the xerogels of **1a** and **1b** from toluene aggregated into a fibrillar self-assembly with fiber diameters of 100–150 nm and lengths of several dozens of micrometers. Similarly, the entangled fibrillar network morphologies of thicker fibers with 200–300 nm in diameter in which a few of fibers linked with each other were observed for the xerogels of **1a** and **1b** obtained from CHCl₃/*n*-hexane (6:5 for **1a** and 2:1 for **1b**, v/v) (Figure 4c and d). By comparison, **1a** and **1b** in the solvent mixture of DMSO/water (2:1, v/v) self-aggregated into a rod-type self-assembly with 0.1–0.5 μm in width and more than 100 μm in length, which is a few of slim rods as seen in Figure 4e and f. Notably, the rod-like translucent gel without thermal treatment transformed into an opaque gel when subjected to heating and cooling

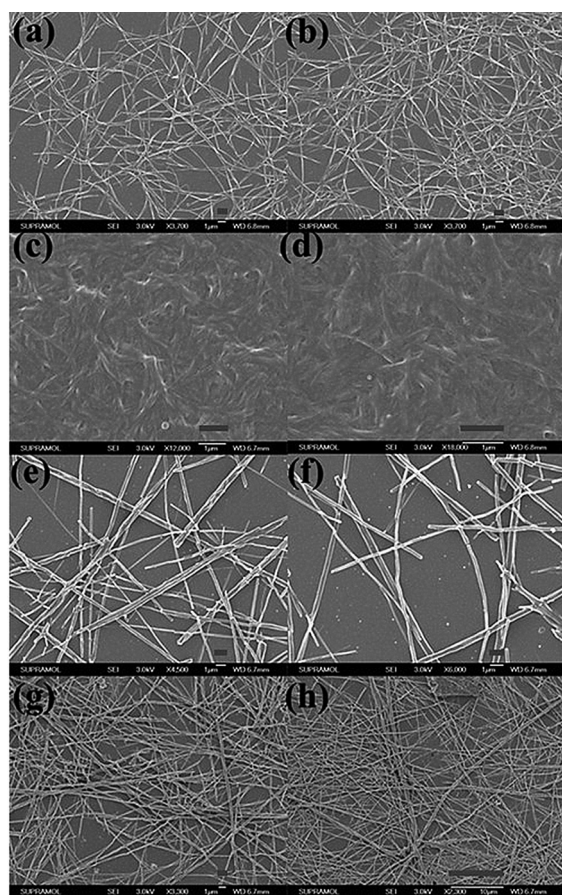


Figure 4. The SEM images of the xerogels obtained from **1 a** (a) and **1 b** (b) from toluene; **1 a** (c) and **1 b** (d) from CHCl_3/n -hexane; **1 a** (e) and **1 b** (f) with or **1 a** (g), and **1 b** (h) without thermal treatment from DMSO/water. The scale bars correspond to $1\ \mu\text{m}$ (a, b, c, d, e, f, g) and $10\ \mu\text{m}$ (h), respectively.

process but no microscopic structures of the gel system was found (Figure 4 g and h).

SAXS study

To understand the molecular packing pattern of the dendrons in gel phase, the X-ray diffraction patterns of the xerogels of gelator **1 b** from toluene and DMSO/water (without thermal treatment) were analyzed. In both cases, the diffraction patterns are characterized by two reflection peaks in the small-angle region. In the case of xerogel obtained from toluene, two reflection peaks of scattering pattern was observed at 2.6 and 1.86 nm in the small-angle region with a scattering vector ratio of $1:\sqrt{2}$, corresponding to a 2D rectangular structure with $a=2.6\ \text{nm}$ and $b=1.31\ \text{nm}$, as shown in Figure 5a. Similarly, the xerogel obtained from a mixture of DMSO/water also self-aggregated to a 2D rectangular structure (Figure 5b). In both cases, the average number of dendrons in a disk was calculated to be approximately 1 based on calculations using the Equation in ref. [23]. In addition, considering that the molecular length was approximately 2.55 nm (based on the CPK model), the molecules have a monomolecular arrangement in the matrix. On the basis on these results, we assumed that the

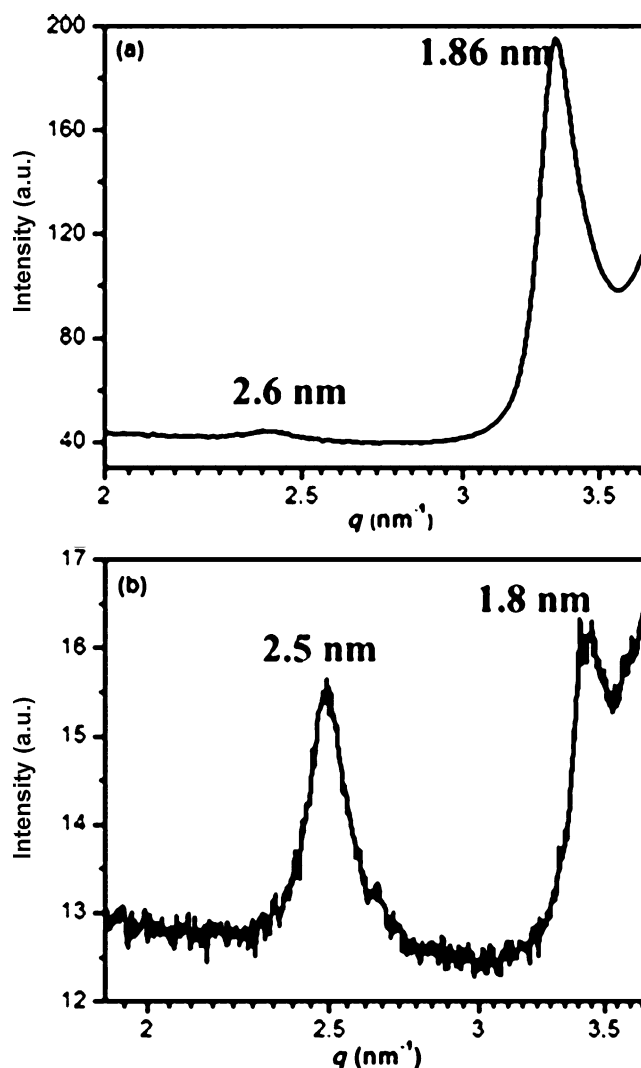


Figure 5. SAXS patterns of xerogels of **1 b** from toluene (a) and DMSO/water (2:1, v/v) without thermal treatment (b).

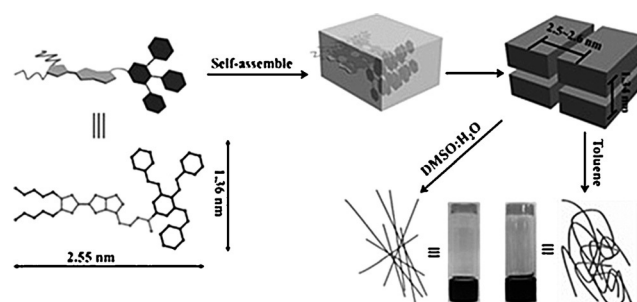


Figure 6. Cartoon representation of the self-assembly of **1 b** in the both cases.

molecule might favor packing in a parallel fashion to maximize π -stacking, hydrogen-bonding, and $\text{S}\cdots\text{S}$ interactions.^[36] The packing model of the rectangular columnar phase is shown in Figure 6.

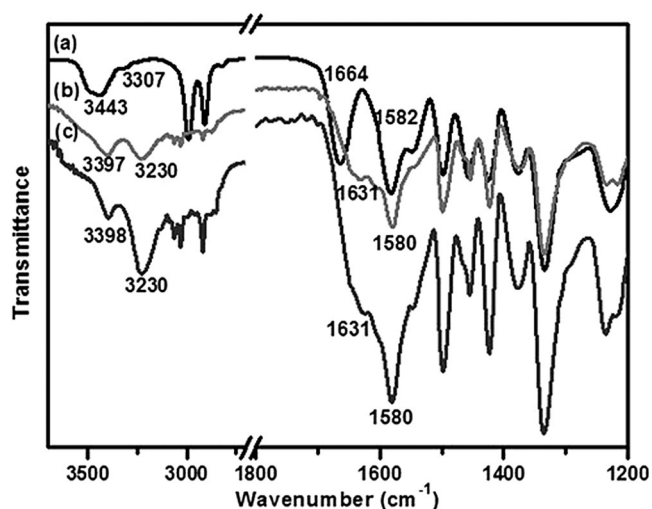


Figure 7. FTIR spectra of **1a** in DMSO solution (a), xerogel from toluene (b) and CHCl_3/n -hexane (6:5, v/v, c).

Driving-force study

Fourier transform infrared spectroscopy (FTIR) is a powerful tool to study noncovalent interactions, especially hydrogen bonding in the gelation.^[37] To find out the involvement of acyl hydrazone moieties in dendron molecule in the self-assembly, FTIR spectra of xerogels (from toluene and CHCl_3/n -hexane) and the non-gelated DMSO solution (about 5%) of gelator **1a** were recorded. As shown in Figure 7, the FTIR spectrum of **1a** in DMSO solution shows a broad transmission band at 3443 cm^{-1} which was assigned to ν N–H on nitrogen of the pyrrole ring and a narrow band at 3282 cm^{-1} due to non-hydrogen-bonded ν N–H (amide A) as well as other two bands at 1664 and 1582 cm^{-1} , the latter bands are characteristic of ν C=O (amide I) and δ N–H (amide II) frequencies, respectively. However, in the FTIR spectra of the xerogels both from toluene and CHCl_3/n -hexane, the correspondent amide A and amide I were redshifted by 52 and 33 cm^{-1} , respectively, whereas amide II was slightly blueshifted by 2 cm^{-1} . A noticeable change in FTIR spectrum is that the transmission band of N–H on nitrogen of pyrrole ring in gels was also redshifted about 46 cm^{-1} with respect to the DMSO solution. These change of transmission bands indicate the involvement of hydrogen bonding from amide group and, in particular, the N–H bond of pyrrole ring in the gelation process. Similar FTIR spectral changes were also observed for gelator **1b** under same experimental conditions (the Supporting Information, Figure S2).

To clarify the existence of noncovalent interaction in the self-assembled network, taking **1b** (5.0 mg mL^{-1} in C_6D_6) as an example, temperature-dependent ^1H NMR experiment was performed (the Supporting Information, Figure S3). Because of the strong self-assembly and the opaque gel state at room temperature, no obvious signals of amide NH, pyrrole NH and $-\text{CH}=\text{N}-$ were detected, and other proton signals presented broad peaks, such as pyrrole CH and the alkyl residue. Upon heating from 293 K (gel state) to 353 K (solution state), the peaks ascribed to the amide NH, pyrrole NH and $-\text{CH}=\text{N}-$

started to appear and became gradually sharper and stronger and the original broad peaks also became gradually sharper and stronger with increasing temperature. A broad peak for amide NH and pyrrole NH could be found at $\delta = 8.38\text{ ppm}$ over 323 K , which was split and shifted upfield gradually to $\delta = 8.40$ and 8.12 ppm , respectively. Another peak for the $-\text{CH}=\text{N}-$ unit appeared at $\delta = 7.57\text{ ppm}$ and shifted downfield to $\delta = 7.62\text{ ppm}$. In the same way, the weak and broad signals for pyrrole CH and aryl ether CH_2O became gradually sharper and stronger with increasing temperature and shifted downfield from $\delta = 5.81$ and 4.85 ppm to 5.83 and 4.91 ppm , respectively. Furthermore, the signals from the protons on the alkyl segment were shifted downfield by about 0.047 – 0.083 ppm and the signals of the benzene rings in the range of $\delta = 7.47$ – 7.00 ppm showed slight upfield shifts ($<0.01\text{ ppm}$). The NMR result revealed that supramolecular aggregates were formed through intermolecular hydrogen bonding, π – π and van der Waals interactions of gelator molecules.

To gain further insight into the hydrogen bonding is one of the main driving forces for gelation, we subsequently examined the stimuli-responsive property of gel of **1a** in toluene towards the various anions (as the tetrabutylammonium salt). As seen in Figure 8a and Figure S4 (the Supporting Information), upon addition of 3.0 equiv of F^- , Cl^- or AcO^- , as time passed, the gel gradually transformed into a yellow solution but the color of the sol formed had no a drastic change in the whole process (the Supporting Information, Figure S5), suggesting that the collapse of gel phase arise from the anion-binding interactions rather than the deprotonation. The gel could be adversely preserved upon addition of the same amount of other anions (Br^- , I^- , H_2PO_4^- , HSO_4^-). In addition, the gel could not be restored by adding the protic solvents (such as methanol or H_2O), which provides another evidence for the aforementioned mechanism. However, the gel obtained from DMSO/ H_2O could not be destroyed upon addition of anions. Additional evidence

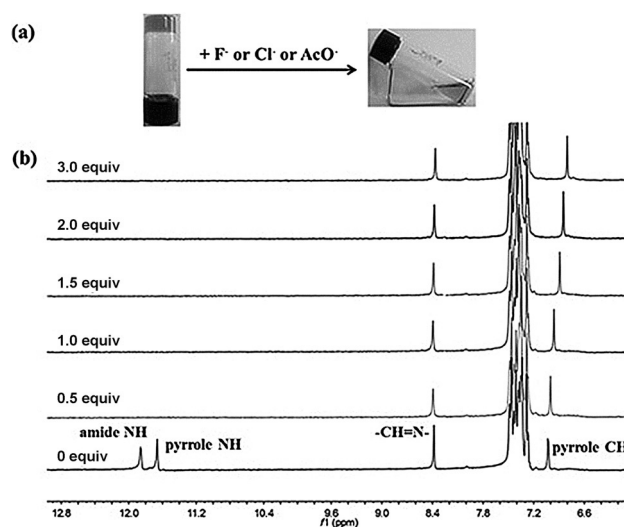


Figure 8. (a) Photographs of the gel-sol and color transitions of **1a** in toluene in the presence of 3.0 equiv F^- or Cl^- or AcO^- and (b) ^1H NMR ($[\text{D}_6]\text{DMSO}$) spectra of **1a** in the presence of F^- in $[\text{D}_6]\text{DMSO}$.

for the stimuli-responsive mechanism was obtained from ^1H NMR experiments in $[\text{D}_6]\text{DMSO}$. The peaks of the amide N–H, pyrrole N–H, pyrrole –CH– and –CH=N– protons in gelator **1a** appeared at $\delta = 11.87$, 11.68 and 7.04 and 8.40 ppm, respectively. After adding 0.5 equiv of F^- , the peaks at $\delta = 11.87$ and 11.68 ppm for the proton of amide unit and the proton on nitrogen of pyrrole, respectively, disappeared, but no peak was observed for the HF_2^- anion around $\delta = 16$ ppm, which further supported the anion-binding mechanism. Upon treatment with the increasing amounts of F^- , the peak at $\delta = 7.04$ for the proton of pyrrole ring was shifted upfield to $\delta = 6.80$ ppm, probably because of the enhanced self-assembly through π – π interactions (Figure 8b). Moreover, addition of anions to DMSO solution of **1a** caused hardly any significant spectral change (the Supporting Information, Figure S6), which also refuted the deprotonation mechanism.

Next, to prove the π – π interactions between aromatic moieties during gelation, the UV/Vis spectra of **1a** both in the dilute toluene solution (5×10^{-5} M) and xerogel state were recorded. In dilute solution, gelator **1a** showed a strong absorption band at 346 nm, which was attributed to the π – π^* transitions of the molecular backbone. As for the xerogel state, this band took an obvious redshift to 350 nm and accompanied with the decrease of the intensity. This result suggested that J-aggregates were formed in the toluene gel. The UV/Vis absorption spectra for gelator **1a** in DMSO were also recorded with addition of increasing amounts of H_2O at room temperature. As shown in Figure 9b, gelator **1a** in DMSO solution (5×10^{-5} M) showed two absorption bands centered at 267 and 346 nm, which could be ascribed to the π – π^* transitions of the MPTTF and conjugated molecular backbone, respectively. When increasing the water content to 33.3% (2:1, v/v), these two absorption bands redshifted to 303 and 358 nm, respectively. By increasing the water content further to 66.7% (1:2, v/v), the band at 346 nm continued to redshift to 369 nm and resulted in an obvious Tyndall phenomenon (the Supporting Information, Figure S7), indicative of the formation of J-aggregates within self-assembly process. There is no doubt that the π – π interactions plays a key role in the gelation process.^[33b,38] On the other hand, as seen from the optimized structure (the Supporting Information, Figure S8), the MPTTF and dendron unit in the respective plane provide a favorable environment for π – π stacking between molecules.

The electrochemical properties of the gelators and the corresponding gels were evaluated by cyclic voltammetry in toluene/acetonitrile (v/v = 4:1, 0.5 mm, vs. Ag/AgCl). Taking gelator **1a** as example, as shown in Figure 10a, the solution of **1a** showed two reversible single-electron oxidation waves at approximately $E = +0.587$ V (I), $+0.938$ V (II), which were assigned to the formation of radical cation and dication of TTF, respectively.^[39] By comparison, the xerogel of **1a** from toluene exhibited two quasi-reversible oxidation waves at 0.562 and 0.913 V, (Figure 10b), respectively, and both were negatively shifted by 0.025 V compared with those in solution under the same conditions. The lower oxidation potentials of the TTF gel phase should be attributed to the stabilization effect arising from the strong π – π and S...S interactions.^[31a]

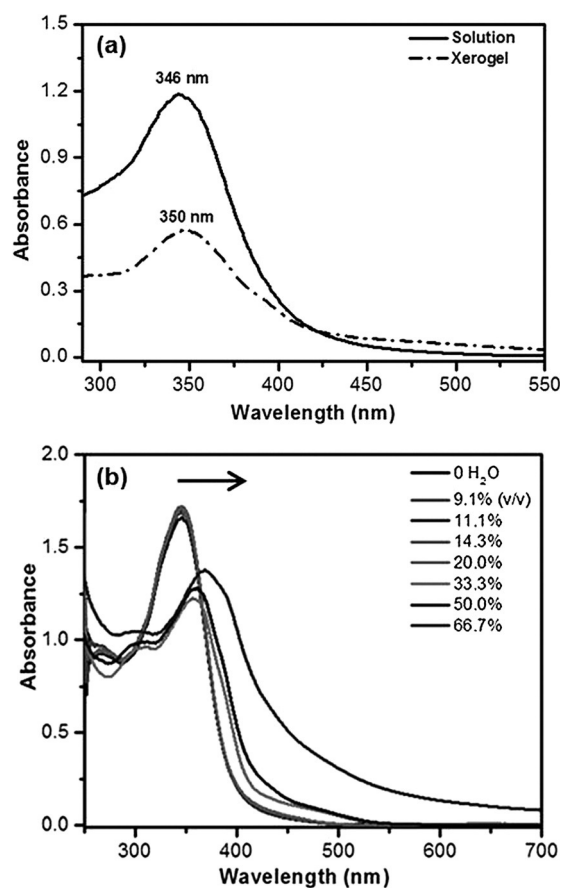


Figure 9. UV/Vis spectra of **1a** (a) of the dilute toluene solution (5×10^{-5} M) and xerogel from toluene and (b) in DMSO (5×10^{-5} M) with addition of increasing amounts of H_2O at room temperature.

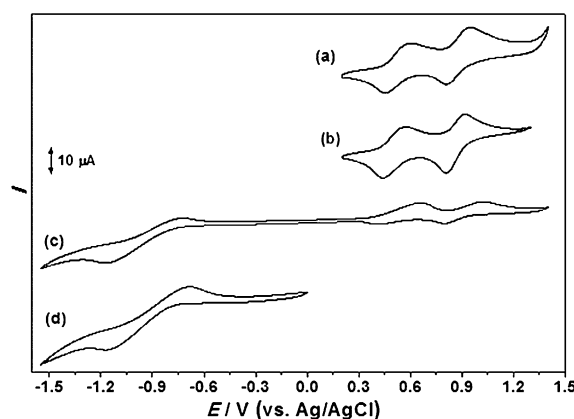


Figure 10. Cyclic voltammograms of (a) **1a** solution (0.5 mM); (b) native xerogel of **1a** from toluene; (c) binary xerogel of **1a** with C_{60} from toluene; and (d) C_{60} (0.25 mM) in toluene/ CH_3CN (4:1, v/v). Containing 0.1 M Bu_4NPF_6 and the scan rate was 100 mV s^{-1} .

Chemical redox

As we know, the TTF moiety could be oxidized in an oxidative environment, leading to the gel's response to certain external chemical stimuli. When an equivalent amount of $\text{Fe}(\text{ClO}_4)_3$ was carefully placed above the gel of **1a** in toluene, the gel gradu-

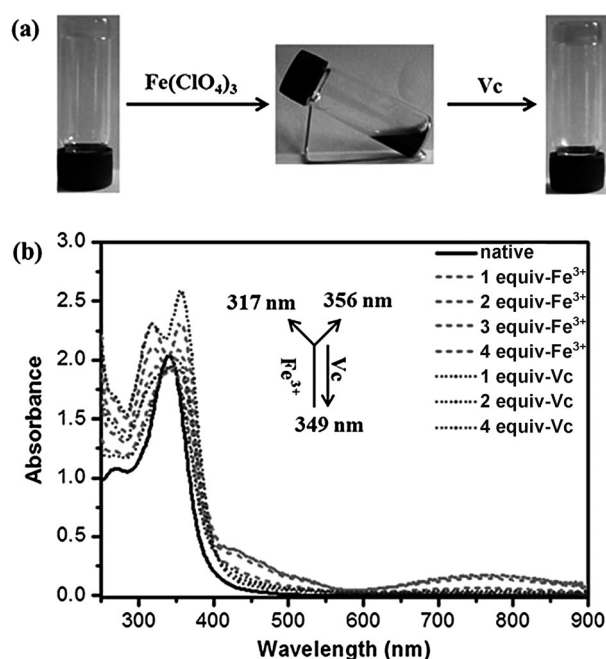


Figure 11. (a) The gel–sol transitions of the gel of **1 a** by chemical redox reaction in toluene, and (b) the corresponding changes of UV/Vis spectra of **1 a** upon chemical redox in THF/CHCl₃ (5×10^{-5} M, 1:1, v/v).

ally turned into a dark-green solution (Figure 11a).^[31] The mechanism of phase transition is identical to that observed during electrochemical oxidation, that is, TTF was oxidized to TTF⁺, which results in the repulsion between the MPTTF units to destroy the π - π and S...S interactions between TTF units, and thereby the gel network collapses.^[18] Notably, when an equivalent ascorbic acid (Vitamin C, Vc) dissolved in small amount of water was added to the oxidized solution, which was able to reduce TTF⁺ to the neutral TTF, the organogel reformed upon cooling the hot solution. Such a gel–sol transition could be repeated for several cycles. Further evidence for redox reaction processes was monitored by a UV/Vis spectroscopy. The UV/Vis spectrum of **1 a** in THF/CHCl₃ (1:1, v/v) did not show any absorption bands in the range of 400 to 900 nm. However, upon addition of increasing amounts of Fe³⁺, the peak assignable to dendron molecular backbone absorption (at 349 nm) was split into two peaks at 317 and 356 nm. Meanwhile, two new absorption peaks centered at 429 and 760 nm emerged, respectively, which were assigned to the absorption bands of MPTTF⁺.^[33b,40] In turn, the two characteristic bands assignable to the MPTTF⁺ cation gradually decreased with the increase in Vc concentration. Finally, the original spectrum of **1 a** was totally regenerated upon the addition of 4 equivalents of Vc (Figure 11b) and the color of the solution also experienced reversible transformation in the whole redox process (the Supporting Information, Figure S9).

Fluorescence properties of the gels

It is well known that the “aggregation-caused quenching” (ACQ) effect exists in the gel formation process in most cases,

which is become a thorny obstacle to the development of their light-emitting properties.^[41] Recently, aggregation-induced emission (AIE) or aggregation-induced enhanced emission (AIEE) have been reported by many scientists in organic molecules with a structural feature of one conjugated stator carrying multiple aromatic peripheral rotors because of the restriction of the intramolecular rotation.^[42] Therefore, the close packing of MPTTF and aromatic units in the dendron will results in the aggregation induced fluorescence emission.^[43] To verify the hypothesis, the fluorescence spectroscopic investigation of the gelator was carried out taking **1 a** as example. Gelator **1 a** is almost non-emissive in neat DMSO solution when excited at 346 nm. Addition of 33% water (2:1, v/v) to the DMSO solution of **1 a** results in the gelation and elicited a big fluorescence enhancement (≈ 240 fold) at 549 nm. The remarkable fluorescence enhancement can be explained by gel-induced enhanced emission (GIEE). The gelation of **1 a** in toluene similarly induces 100 fold fluorescence enhancement as compared with the DMSO solution (Figure 12a). It is interesting that the change of the fluorescence emission of the system is easily to survey due to that the gelation in DMSO/water mixture does not need the heating and cooling process. To further understand the role of π - π stacking for the emission nature of gel state, therefore, the fluorescence emission change of **1 a** in the sol–gel transition was tracked by gradual addition of water to the DMSO solution (0 to 33.3%, v/v). As shown in Figure 12b, with gradual addition of water to the DMSO solution, the emission intensity of **1 a** gradually increased. When addition about 11% of water, the system started to elicit fluorescence emission at about 500 nm. With an increase of water content, the emission wave gradually shifts to 549 nm, showing the GIEE phenomenon occurred. Note that when the water content reached 25%, a sudden change of the emission intensity was observed, and a maximal fluorescent signal is achieved until the water content reached 29.4%. However, the emission intensity at 549 nm was slightly decreased along with increase the water content (33.3%) likely due to the lower transparency of the gel (the Supporting Information, Figure S10).

On the other hand, gelator **1 a** showed concentration-dependent emission property in toluene. Upon increasing the concentration of **1 a** from 0.4 to 2.0 mg mL⁻¹, the emission intensity at 549 nm gradually increased and accompanied by the gelation (Figure 12c). The time-dependent change of the fluorescence intensity was also investigated in toluene (1.6 mg mL⁻¹) (Figure 12d). The fluorescence emission of **1 a** in the hot toluene solution exhibited a negligibly small emission intensity. With the aging time at room temperature, the emission intensity of 549 nm was gradually strengthened. When the hot toluene solution of **1 a** was naturally cooled for 12 min, the process of sol–gel transition was finished and the emission intensity of the gel was almost reached the maximum. Note that at early stage of gelation, the initial fluorescence silence was observed (<1.8 min) and then, fluorescence emission intensity increased drastically and finally reached a maximum value.^[44] The above results proved further that the π - π interactions is a the main driving force.

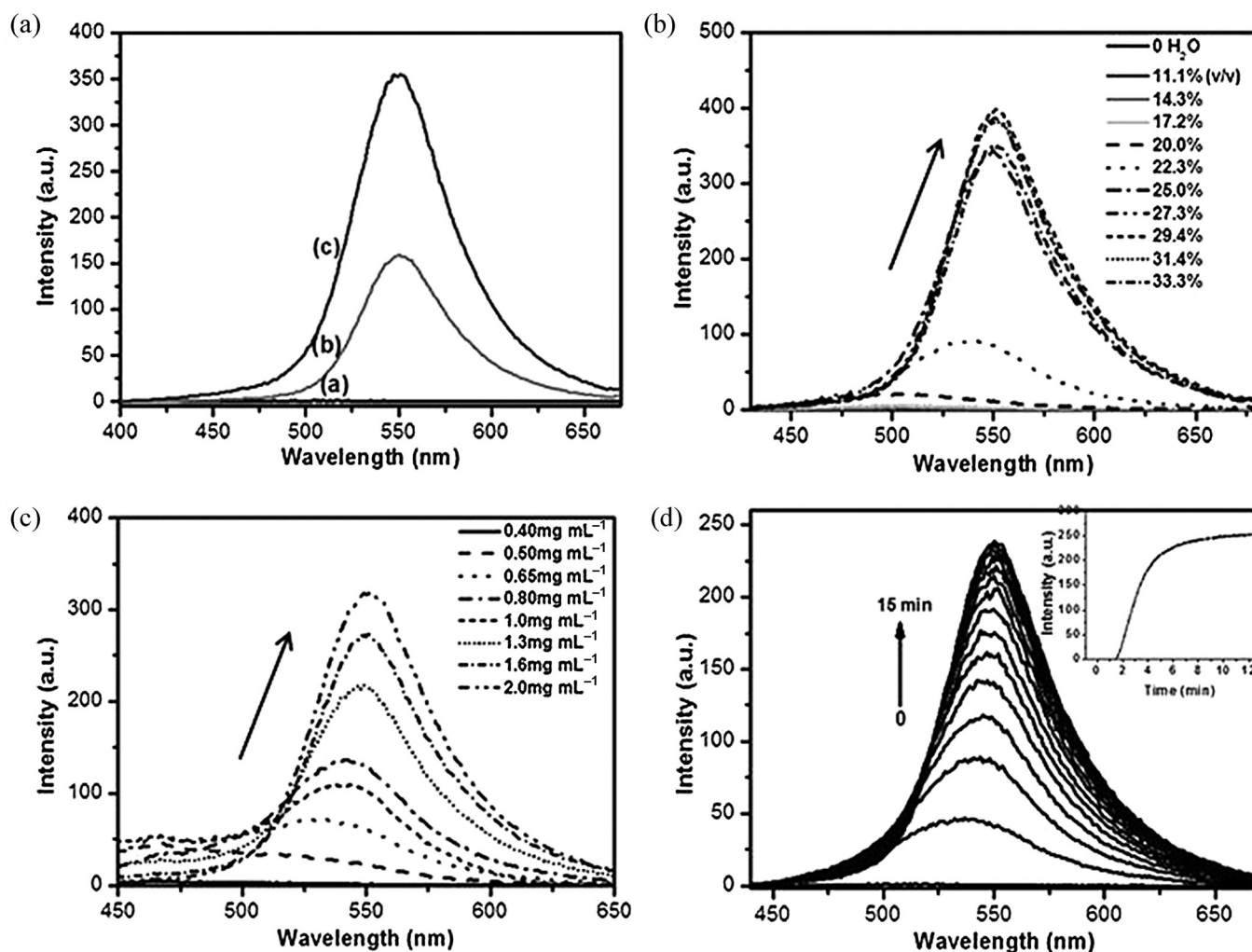


Figure 12. Fluorescence spectra of compound **1a** (A) in DMSO solution (a), the gel in toluene (b, 1.6 mg mL^{-1}) and DMSO/water (c, 0.8 mg mL^{-1} , 2:1, v/v); (B) in DMSO (2.25 mg mL^{-1}) with addition of different amount of H₂O; (C) in toluene with increasing of the concentration and (D) of the time-dependent changes in toluene (1.6 mg mL^{-1}). The inset is the fluorescent time sweep experiment for the gel of **1a** from toluene.

Binary organogel formation with C₆₀

TTF and its derivatives have received considerable attention as donor components in the molecular assembly because they have strong electron-donating ability.^[21a,25,45] It is expected that the π - π and S...S interactions in the gel phase would be destroyed by introduction of an acceptor molecules, such as C₆₀, through the intermolecular charge-transition (CT) interactions. Contrary to expectations, when different amounts of C₆₀ (from 0~1 equiv) dissolved in toluene were placed above the gels of **1a** in toluene, a dark-brown gel was formed upon heating and cooling process (Figure 13). To determine the optimum stoichiometry for the gel, T_{gel} was measured with increasing amounts of C₆₀ at a constant concentration of **1a**. A plot of T_{gel} versus the molar ratio of C₆₀ showed a maximum value of T_{gel} at a 2:1 molar ratio (Figure 13). The results suggested that two MPTTF moieties in **1a** bind with one C₆₀ molecule to form a 2:1 **1a**/C₆₀ sandwich-type complex (Figure 14).^[46] To explore the driving-force in the gel, the electron paramagnetic resonance spectrum was recorded at 298 K but no electron spin resonance (ESR) signal was observed in the region characteristic of

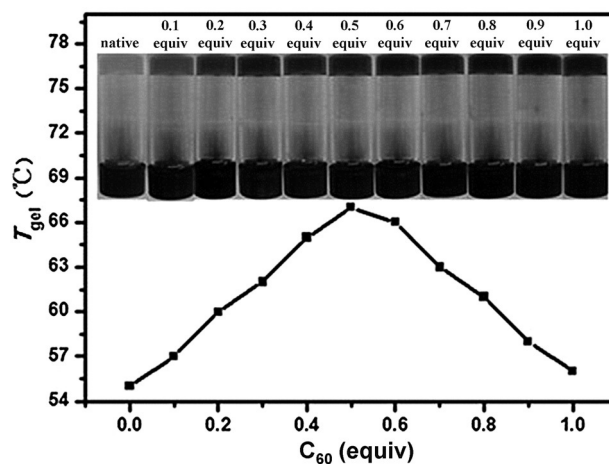


Figure 13. Variation of the gel melting temperature of **1a** (2.0 mg mL^{-1}) with different amounts of C₆₀ (from 0 to 1.0 equiv) in the toluene; the inset shows the color change for the gels based on compound **1a** after addition of different amounts of C₆₀.

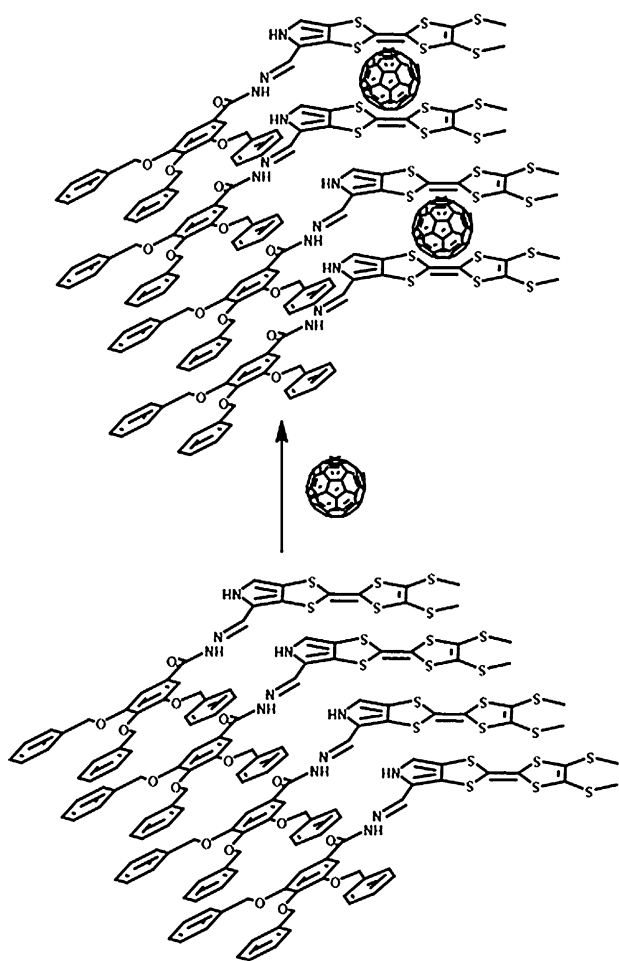


Figure 14. Cartoon representation of the possible molecular packing mode for **1a** in the gel with C_{60} .

the TTF radical cation (the Supporting Information, Figure S11), indicative of that the formed gel is not a charge-transfer (CT) complex gel but a binary gel, which is derived by intermolecular interactions. On the other hand, the change of redox potential of the binary xerogel from toluene supported further the intermolecular interaction mechanism. The binary gel from toluene/acetonitrile ($v/v = 4:1$) mixture exhibits two quasi-reversible oxidation waves at 0.656 and 1.017 V (Figure 10c), respectively, which were far higher than those of the native gel of **1a**, and an irreversible reduction wave at -1.169 V that is 10 mV more negative than that of C_{60} itself in toluene/acetonitrile mixture. The features of optical absorption of the binary gels containing different amounts of C_{60} confirmed further the absence of CT complex (the Supporting Information, Figure S12). These results are in agreement with our proposed interaction mechanism.

Interestingly, an evident change took place in the morphology of the binary gel compared with those of the corresponding native gel. The fibrous morphology of the native gel of **1a** obtained from toluene transformed into the elliptical morphology, which consists of many short rod-like structures (Figure 15a). The coexistence of C_{60} , which is an electron-acceptor, in binary gel will inevitably cause the

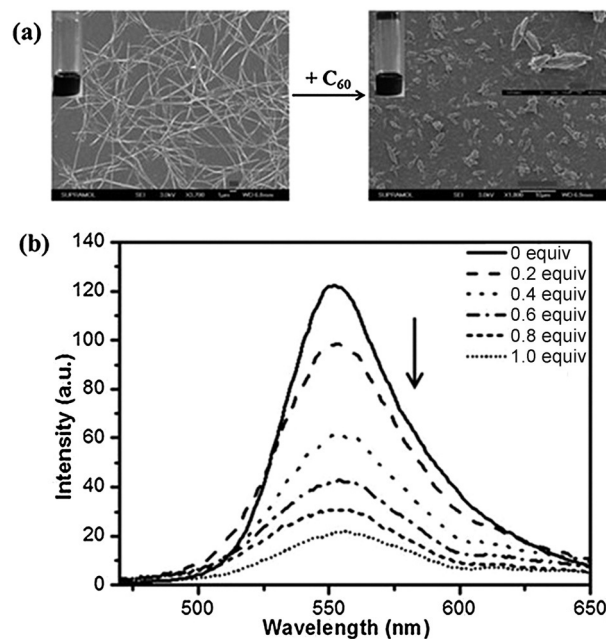


Figure 15. (a) The SEM images of the binary gel of **1a** after adding C_{60} (mole ratio = 1:0.5) and (b) Fluorescence quenching of organogel **1a** from toluene upon titration with C_{60} . The scale bars correspond to (left and the inset of right) $1 \mu\text{m}$ and (right) $10 \mu\text{m}$, respectively.

change of the optical property of the gel. To verify this hypothesis, the emission intensity is monitored as a function of added C_{60} in toluene. As shown in Figure 15b, the emission intensity of the gel system was quenched dramatically by addition of increasing amounts of C_{60} (ca., 5 fold). A similar observation was made for the binary gel of gelator **1b** under same experimental condition (the Supporting Information, Figure S13).

Conclusion

We have developed a new series of low-molecular mass organogelators based on poly(aryl ether) dendron with a monopyrrolotetrathiafulvalene unit. Dendrons **1a** and **1b** with a hydrogen atom on the nitrogen in pyrrole ring could gel aromatic solvents and the mixed solvents to form the thermo-reversible stable gels with low critical gelation concentration. By comparison, dendrons **1c** and **1d** with a methyl group on the nitrogen in pyrrole ring could not gel all solvents tested except for *n*-pentanol. It is interesting to note that the dendrons could form the stable gel in the DMSO/water mixture without thermal treatment and could form the binary gel with C_{60} in toluene. The formation of the binary gel is attributed to the intermolecular interaction between the MPTTF unit and C_{60} , which is confirmed by absorption and ESR spectral studies. The formed gels undergo a reversible gel-sol phase transition upon exposure to external stimuli, such as temperature and chemical oxidation/reduction. The cooperation of hydrogen bonding, π - π and $S \cdots S$ interactions was determined to be the main driving force for the formation of the gels. Moreover, the gel system exhibits gel-induced enhanced emission (GIEE) property in the visible region, despite the absence of a conven-

tional fluorophore unit, and the fluorescence was effectively quenched by introduction of C₆₀. The present gelators with excellent gelation ability, GIEE property and the inherent electronic properties of TTF, it may thus provide important insight into the relevant applications, such as light-harvesting systems and nano-optoelectronic devices.

Acknowledgements

The authors acknowledge financial support from the National Natural Science Foundation of China (grant no. 21262038).

Keywords: dendrons · gels · fluorescence · redox chemistry · self-assembly

- [1] a) T. Aida, E. W. Meijer, S. I. Stupp, *Science* **2012**, *335*, 813–817; b) V. J. Nebot, J. J. Ojeda-Flores, J. Smets, S. Fernández-Prieto, B. Escuder, J. F. Miravet, *Chem. Eur. J.* **2014**, *20*, 14465–14472.
- [2] a) D. K. Smith, *Chem. Soc. Rev.* **2009**, *38*, 684–694; b) J. A. Foster, J. W. Steed, *Angew. Chem. Int. Ed.* **2010**, *49*, 6718–6724; *Angew. Chem.* **2010**, *122*, 6868–6874; c) G. Yu, X. Yan, C. Han, F. Huang, *Chem. Soc. Rev.* **2013**, *42*, 6697–6722; d) C. Tomasini, N. Castellucci, *Chem. Soc. Rev.* **2013**, *42*, 156–172; e) M. D. Segarra-Maset, V. J. Nebot, J. F. Miravet, B. Escuder, *Chem. Soc. Rev.* **2013**, *42*, 7086–7098; f) S. S. Babu, V. K. Praveen, A. Ajayaghosh, *Chem. Rev.* **2014**, *114*, 1973–2129; g) R. G. Weiss, *J. Am. Chem. Soc.* **2014**, *136*, 7519–7530.
- [3] a) F. Zhao, M. L. Ma, B. Xu, *Chem. Soc. Rev.* **2009**, *38*, 883–891; b) J. Li, Y. Kuang, Y. Gao, X. Du, J. Shi, B. Xu, *J. Am. Chem. Soc.* **2013**, *135*, 542–545.
- [4] a) V. Jayawarna, M. Ali, T. A. Jowitt, A. F. Miller, A. Saiani, J. E. Gough, R. V. Uljin, *Adv. Mater.* **2006**, *18*, 611–614; b) A. R. Hirst, B. Escuder, J. F. Miravet, D. K. Smith, *Angew. Chem. Int. Ed.* **2008**, *47*, 8002–8018; *Angew. Chem.* **2008**, *120*, 8122–8139.
- [5] a) J. H. Holtz, S. A. Asher, *Nature* **1997**, *389*, 829–832; b) D. T. McQuade, A. E. Pullen, T. M. Swager, *Chem. Rev.* **2000**, *100*, 2537–2574; c) Z. Hu, X. Zhang, Y. Li, *Science* **1995**, *269*, 525–527; d) Y. Osada, H. Okuzaki, H. Hori, *Nature* **1992**, *355*, 242–244.
- [6] a) N. M. Sangeetha, S. Bhat, G. Raffy, C. Belin, A. Loppinet-Serani, C. Aymonier, P. Terech, U. Maitra, J.-P. Desvergne, A. Del Guerso, *Chem. Mater.* **2009**, *21*, 3424–3432; b) T. Kar, S. Dutta, P. K. Das, *Soft Matter* **2010**, *6*, 4777–4787.
- [7] a) S. R. Jadhav, P. K. Vemula, R. Kumar, S. R. Raghavan, G. John, *Angew. Chem. Int. Ed.* **2010**, *49*, 7695–7698; *Angew. Chem.* **2010**, *122*, 7861–7864; b) S. Mukherjee, C. Shang, X. Chen, X. Chang, K. Liu, C. Yu, Y. Fang, *Chem. Commun.* **2014**, *50*, 13940–13943.
- [8] a) D. Das, S. Roy, S. Debnath, P. K. Das, *Chem. Eur. J.* **2010**, *16*, 4911–4922; b) N. Bruns, J. C. Tiller, *Nano Lett.* **2005**, *5*, 45–48.
- [9] D. Díaz Díaz, D. Kuhbeck, R. J. Koopmans, *Chem. Soc. Rev.* **2011**, *40*, 427–448.
- [10] D. K. Kumar, J. W. Steed, *Chem. Soc. Rev.* **2014**, *43*, 2080–2088.
- [11] Y. He, M. Xu, R. Gao, X. Li, F. Li, X. Wu, D. Xu, H. Zeng, L. Yuan, *Angew. Chem. Int. Ed.* **2014**, *53*, 11834–11839; *Angew. Chem.* **2014**, *126*, 12028–12033.
- [12] Y. Feng, Y.-M. He, Q.-H. Fan, *Chem. Asian J.* **2014**, *9*, 1724–1750.
- [13] a) D. K. Smith, *Adv. Mater.* **2006**, *18*, 2773–2778; b) M. A. Carnahan, C. Middleton, J. Kim, T. Kim, M. W. Grinstaff, *J. Am. Chem. Soc.* **2002**, *124*, 5291–5293; c) M. Wathier, P. J. Jung, M. A. Carnahan, T. Kim, M. W. Grinstaff, *J. Am. Chem. Soc.* **2004**, *126*, 12744–12745.
- [14] a) Y. Feng, Z.-T. Liu, J. Liu, Y.-M. He, Q.-Y. Zheng, Q.-H. Fan, *J. Am. Chem. Soc.* **2009**, *131*, 7950–7951; b) Q. Chen, Y. Feng, D. Zhang, G. Zhang, Q. Fan, S. Sun, D. Zhu, *Adv. Funct. Mater.* **2010**, *20*, 36–42.
- [15] W.-D. Jang, D.-L. Jiang, T. Aida, *J. Am. Chem. Soc.* **2000**, *122*, 3232–3233.
- [16] Q. Chen, D. Zhang, G. Zhang, X. Yang, Y. Feng, Q. Fan, D. Zhu, *Adv. Funct. Mater.* **2010**, *20*, 3244–3251.
- [17] a) P. Rajamalli, E. Prasad, *Soft Matter* **2012**, *8*, 8896–8903; b) P. Rajamalli, S. Atta, S. Maity, E. Prasad, *Chem. Commun.* **2013**, *49*, 1744–1746; c) P. Rajamalli, P. S. Sheet, E. Prasad, *Chem. Commun.* **2013**, *49*, 6758–6760; d) P. Rajamalli, E. Prasad, *Langmuir* **2013**, *29*, 1609–1617; e) P. Rajamalli, E. Prasad, *Org. Lett.* **2011**, *13*, 3714–3717.
- [18] N. V. Lakshmi, D. Mandal, S. Ghosh, E. Prasad, *Chem. Eur. J.* **2014**, *20*, 9002–9011.
- [19] a) T. Kitamura, S. Nakaso, N. Mizoshita, Y. Tochigi, T. Shimomura, M. Moriyama, K. Ito, T. Kato, *J. Am. Chem. Soc.* **2005**, *127*, 14769–14775; b) J. Puigmartí-Luis, Á. Pérez del Pino, E. Laukhina, J. Esquena, V. Laukhin, C. Rovira, J. Vidal-Gancedo, A. G. Kanaras, R. J. Nichols, M. Brust, D. B. Amabilino, *Angew. Chem. Int. Ed.* **2008**, *47*, 1861–1865; *Angew. Chem.* **2008**, *120*, 1887–1891; c) R. J. Kumar, J. M. MacDonald, T. B. Singh, L. J. Waddington, A. B. Holmes, *J. Am. Chem. Soc.* **2011**, *133*, 8564–8573; d) S. Prasanthkumar, A. Gopal, A. Ajayaghosh, *J. Am. Chem. Soc.* **2010**, *132*, 13206–13207.
- [20] a) D. R. Stewart, D. A. A. Ohlberg, P. A. Beck, Y. Chen, R. S. Williams, J. O. Jeppesen, K. A. Nielsen, J. F. Stoddart, *Nano Lett.* **2004**, *4*, 133–136; b) G. Ho, J. R. Heath, M. Kondratenko, D. F. Perepichka, K. Arseneault, M. Pézolet, M. R. Bryce, *Chem. Eur. J.* **2005**, *11*, 2914–2922; c) E. Leary, S. J. Higgins, H. van Zalinge, W. Haiss, R. J. Nichols, S. Nygaard, J. O. Jeppesen, J. Ulstrup, *J. Am. Chem. Soc.* **2008**, *130*, 12204–12205; d) C. R. Parker, Z. Wei, C. R. Arroyo, K. Jennum, T. Li, M. Santella, N. Bovet, G. Zhao, W. Hu, H. S. J. van der Zant, M. Vanin, G. C. Solomon, B. W. Laursen, K. Nørgaard, M. B. Nielsen, *Adv. Mater.* **2013**, *25*, 405–409; e) M. V. Solano, E. A. Della Pia, M. Jevric, C. Schubert, X. Wang, C. van der Pol, A. Kadziola, K. Nørgaard, D. M. Guldi, M. B. Nielsen, J. O. Jeppesen, *Chem. Eur. J.* **2014**, *20*, 9918–9929.
- [21] a) M. Hasegawa, M. Iyoda, *Chem. Soc. Rev.* **2010**, *39*, 2420–2427; b) C. Bejger, J. S. Park, E. S. Silver, J. L. Sessler, *Chem. Commun.* **2010**, *46*, 7745–7747; c) A. Y. Ziganshina, Y. H. Ko, W. S. Jeon, K. Kim, *Chem. Commun.* **2004**, 806–807; d) M. Bendikov, F. Wudl, D. F. Perepichka, *Chem. Rev.* **2004**, *104*, 4891–4946.
- [22] a) T. Kakinuma, H. Kojima, T. Kawamoto, T. Mori, *J. Mater. Chem. C* **2013**, *1*, 2900–2905; b) N. M. Tucker, A. L. Briseno, O. Acton, H.-L. Yip, H. Ma, S. A. Jenekhe, Y. Xia, A. K. Y. Jen, *ACS Appl. Mater. Interfaces* **2013**, *5*, 2320–2324; c) L. Tan, Y. Guo, Y. Yang, G. Zhang, D. Zhang, G. Yu, W. Xu, Y. Liu, *Chem. Sci.* **2012**, *3*, 2530–2541; d) M. Mas-Torrent, M. Durkut, P. Hadley, X. Ribas, C. Rovira, *J. Am. Chem. Soc.* **2004**, *126*, 984–985.
- [23] R. Hou, K.-I. Zhong, Z. Huang, L. Y. Jin, B. Yin, *Tetrahedron* **2011**, *67*, 1238–1244.
- [24] H. Lu, W. Xu, D. Zhang, D. Zhu, *Chem. Commun.* **2005**, 4777–4779.
- [25] D. Canevet, M. Salle, G. Zhang, D. Zhang, D. Zhu, *Chem. Commun.* **2009**, 2245–2269.
- [26] J. Puigmartí-Luis, A. Minoia, S. Lei, V. Geskin, B. Li, R. Lazzaroni, S. De Feyter, D. B. Amabilino, *Chem. Sci.* **2011**, *2*, 1945–1951.
- [27] a) A. I. de Lucas, N. Martín, L. Sánchez, C. Seoane, R. Andreu, J. Garín, J. Orduna, R. Alcalá, B. Villacampa, *Tetrahedron* **1998**, *54*, 4655–4662; b) M. González, N. Matín, J. Segura, J. Garín, J. Orduna, *Tetrahedron Lett.* **1998**, *39*, 3269–3272; c) M. González, N. Martín, J. Segura, C. Seoane, J. Garín, J. Orduna, R. Alcalá, C. Sánchez, B. Villacampa, *Tetrahedron Lett.* **1999**, *40*, 8599–8602.
- [28] N. Martín, L. Sánchez, M. Á. Herranz, B. Illescas, D. M. Guldi, *Acc. Chem. Res.* **2007**, *40*, 1015–1024.
- [29] M. Joergensen, K. Bechgaard, T. Bjoernholm, P. Sommer-Larsen, L. G. Hansen, K. Schaumburg, *J. Org. Chem.* **1994**, *59*, 5877–5882.
- [30] T. Akutagawa, K. Kakiuchi, T. Hasegawa, S.-i. Noro, T. Nakamura, H. Hasegawa, S. Mashiko, J. Becher, *Angew. Chem. Int. Ed.* **2005**, *44*, 7283–7287; *Angew. Chem.* **2005**, *117*, 7449–7453.
- [31] a) C. Wang, D. Zhang, D. Zhu, *J. Am. Chem. Soc.* **2005**, *127*, 16372–16373; b) C. Wang, Q. Chen, F. Sun, D. Zhang, G. Zhang, Y. Huang, R. Zhao, D. Zhu, *J. Am. Chem. Soc.* **2010**, *132*, 3092–3096.
- [32] X. Yang, G. Zhang, L. Li, D. Zhang, L. Chi, D. Zhu, *Small* **2012**, *8*, 578–584.
- [33] a) Y. Liu, N. Zheng, H. Li, B. Yin, *Soft Matter* **2013**, *9*, 5261–5269; b) Y. Liu, N. Zheng, T. Chen, L. Jin, B. Yin, *Org. Biomol. Chem.* **2014**, *12*, 6927–6936.
- [34] a) J. O. Jeppesen, K. Takimiya, F. Jensen, T. Brimert, K. Nielsen, N. Thorup, J. Becher, *J. Org. Chem.* **2000**, *65*, 5794–5805; b) C. An, R. Hou, H. Qiu, L. Zhao, B. Yin, Z. Su, *Chin. J. Appl. Chem.* **2009**, *26*, 795–800.
- [35] E. Dahan, P. R. Sundararajan, *Soft Matter* **2014**, *10*, 5337–5349.
- [36] J.-H. Ryu, L. Tang, E. Lee, H.-J. Kim, M. Lee, *Chem. Eur. J.* **2008**, *14*, 871–881.

- [37] T. Kar, S. Mukherjee, P. K. Das, *New J. Chem.* **2014**, *38*, 1158–1167.
- [38] T. Kunitake, *Angew. Chem. Int. Ed. Engl.* **1992**, *31*, 709–726; *Angew. Chem.* **1992**, *104*, 692–710.
- [39] Y. Hou, X. Wan, M. Yang, Y. Ma, Y. Huang, Y. Chen, *Macromol. Rapid Commun.* **2008**, *29*, 719–723.
- [40] a) H. Spanggaard, J. Prehn, M. B. Nielsen, E. Levillain, M. Allain, J. Becher, *J. Am. Chem. Soc.* **2000**, *122*, 9486–9494; b) H. Wu, D. Zhang, L. Su, K. Ohkubo, C. Zhang, S. Yin, L. Mao, Z. Shuai, S. Fukuzumi, D. Zhu, *J. Am. Chem. Soc.* **2007**, *129*, 6839–6846; c) J. Liao, J. S. Agustsson, S. Wu, C. Schöenberger, M. Calame, Y. Leroux, M. Mayor, O. Jeannin, Y.-F. Ran, S.-X. Liu, S. Decurtins, *Nano Lett.* **2010**, *10*, 759–764.
- [41] a) X. Cao, L. Meng, Z. Li, Y. Mao, H. Lan, L. Chen, Y. Fan, T. Yi, *Langmuir* **2014**, *30*, 11753–11760; b) C. Shi, Z. Guo, Y. Yan, S. Zhu, Y. Xie, Y. S. Zhao, W. Zhu, H. Tian, *ACS Appl. Mater. Interfaces* **2013**, *5*, 192–198.
- [42] a) Y. Hong, J. W. Y. Lam, B. Z. Tang, *Chem. Soc. Rev.* **2011**, *40*, 5361–5388; b) J. Seo, J. W. Chung, J. E. Kwon, S. Y. Park, *Chem. Sci.* **2014**, *5*, 4845–4850.
- [43] B.-B. Wang, X. Zhang, X.-R. Jia, Y.-F. Luo, Z. Sun, L. Yang, Y. Ji, Y. Wei, *Polymer* **2004**, *45*, 8395–8402.
- [44] Y. Zhang, H. Ding, Y. Wu, C. Zhang, B. Bai, H. Wang, M. Li, *Soft Matter* **2014**, *10*, 8838–8845.
- [45] a) M. B. Nielsen, C. Lomholt, J. Becher, *Chem. Soc. Rev.* **2000**, *29*, 153–164; b) J. L. Segura, N. Martín, *Angew. Chem. Int. Ed.* **2001**, *40*, 1372–1409; *Angew. Chem.* **2001**, *113*, 1416–1455.
- [46] T. Ishi-i, R. Iguchi, E. Snip, M. Ikeda, S. Shinkai, *Langmuir* **2001**, *17*, 5825–5833.

Received: May 25, 2015

Published online on September 7, 2015